Journal of Hazardous Materials Advances 23 (2026) 101424

Contents lists available at ScienceDirect

Journal of Hazardous Materials Advances

journal homepage: www.elsevier.com/locate/hazadv

Attenuation of hazardous metal mobility by mineral based silica system in aqueous environments

Angelo Scarciglia [a,d], Francesco Rosario La Corte [a], Marianna Sorrentino [a], Stefano Marchesi [b], Chiara Bisio [b,e], Fabio Carniato [b,c,**], Enza Di Gregorio [a], Giuseppe Ferrauto [a,*]

[a] Molecular Imaging Center, Department of Molecular Biotechnology and Health Sciences, University of Torino, 10126 Torino, Italy
[b] Dipartimento di Scienze e Innovazione Tecnologica, Università degli Studi del Piemonte Orientale, Viale T. Michel 11, Alessandria, 15121, Italy.
[c] Magnetic Resonance Platform (PRISMA-UPO), Università del Piemonte Orientale, Viale T. Michel 11, 15121 Alessandria, Italy
[d] School of Advanced Defence Studies, Defence Research & Analysis Institute, Piazza della Rovere 83, 00165 Rome, Italy
[e] CNR-SCITEC Istituto di Scienze e Tecnologie Chimiche "Giulio Natta", Via C. Golgi 19, 20133 Milano, Italy.

ARTICLE INFO

Keywords:
Dioptase
Gadolinium
Silicate
^{1}H-NMR Relaxometry
Lanthanides
Magnetic resonance imaging
Rare Earth elements

ABSTRACT

The increasing demand for rare-earth elements (REEs), particularly lanthanides, in industrial, energy, medical, and strategic defense applications has resulted in growing pollution and waste generation worldwide. Gadolinium represents a particularly relevant case study since it is widely used in various industrial and medical field, as the case of Gd^{3+}-based contrast agents for magnetic resonance imaging (MRI), where after MRI scans, GBCAs are excreted through patients' urine, leading to accumulation in rivers, lakes, and seas, with consequent environmental concerns and economic loss. Here we propose a rapid and straightforward approach, using dioptase, a natural copper cyclosilicate mineral, for the recovery and the recycling of REEs. A combined analytical approach based on ^{1}H-NMR-relaxometry and ICP-MS was employed to investigate the adsorption and desorption behavior of dioptase toward La^{3+}, Gd^{3+} and Lu^{3+}, structural integrity of the sorbent was confirmed by XRD, and morphological and spectroscopic properties were characterized using SEM and UV–Visible spectroscopy. Dioptase exhibits a high adsorption capacity for REEs from synthetic aqueous solutions containing free lanthanide ions, achieving 99.6% removal of Gd^{3+} within 7 hours, with adsorption kinetics best described by a parabolic diffusion model (K_d 641.3 mL g^{-1}). Competition experiments revealed a preferential affinity for Lu^{3+} over Gd^{3+} and La^{3+}, likely driven by differences in ionic size and charge density. Desorption experiments under acidic conditions showed efficient metal release, highlighting the reusability of the material. Overall, dioptase emerges as a promising natural sorbent for the recovery of free lanthanide ions from aqueous solutions, thereby contributing to hazardous metal immobilization and circular economy strategies.

Synopsis

This study identifies natural dioptase as an efficient material for recovering rare-earth elements from aqueous media reducing environmental pollution and associated human health risks.

Introduction

Rare earth elements (REEs) are a fundamental class of chemical elements in the Periodic Table, comprising the 15 lanthanides together with scandium and yttrium, which possess unique magnetic, optical and catalytic properties that are considered useful for modern industries and applications in the field of energy storage and rechargeable batteries, strategic military equipment, electronics, high-tech, permanent magnets, and medical imaging (Fig. 1) (Zepf, 2016, Zhang et al., 2022)

The widespread implementation of clean energy technologies is

* Corresponding author at: Molecular Imaging Center, Department of Molecular Biotechnology and Health Sciences, University of Torino, 10126 Torino, Italy.
** Dipartimento di Scienze e Innovazione Tecnologica, Università degli Studi del Piemonte Orientale, Viale T. Michel 11, Alessandria 15121, Italy.
E-mail addresses: fabio.carniato@uniupo.it (F. Carniato), giuseppe.ferrauto@unito.it (G. Ferrauto).

https://doi.org/10.1016/j.hazadv.2026.101424
Received 18 February 2026; Received in revised form 2 July 2026; Accepted 23 July 2026
Available online 24 July 2026
2772-4166/© 2026 The Author(s). Published by Elsevier B.V. This is an open access article under the CC BY license (http://creativecommons.org/licenses/by/4.0/).

driving a substantial increase in the demand for critical minerals and REEs, and as countries intensify their efforts in energy transition, demand for these minerals is also expected to rise significantly. The presence of these metals in specific regions of the world has a strong impact on global strategic discussions, and as industrial activities continues to rise, this poses also significant risks to ecosystems and human health, as in the case of Gd^{3+}-based contrast agents or GBCAs (Scarciglia et al., 2025).

More broadly, the removal of hazardous contaminants from environmental matrices remains one of the major challenges in environmental science. Although considerable research has focused on the remediation of organic pollutants, such as polycyclic aromatic hydrocarbons (PAHs), the fundamental criteria used to evaluate remediation strategies, including efficiency, sustainability, and cost-effectiveness, are equally relevant to the recovery and immobilization of hazardous metals (Hadibarata et al., 2025). In this sense the need for more eco-friendly extraction and better mineral recovery capabilities can promote the development of more sustainable practices that minimize waste and energy consumption, addressing a major economic and environmental challenge (Fei and Hu, 2023, Xu et al., 2024, Mugion et al., 2025). Anthropogenic accumulation of Gd^{3+} chelates has been reported in the environment and water sources, in the proximity of industrial, waste-management and healthcare facilities that produce, process, or use GBCA, e.g. for MRI acquisitions (Dekker et al., 2024, Brünjes and Hofmann, 2020, Kulaksız and Bau, 2011, Kumasaka et al., 2024). Several studies have demonstrated the impact of the biological accumulation of such metals, which have no specific biological function and are often associated with the onset of disorders in animal species (Goff et al., 2019, Martino et al., 2018, Figueiredo et al., 2021) or accumulation and retention in organs with unknown possible effects such as nephrogenic systemic fibrosis (NSF, (Elmholdt et al., 2011)).

Annually more than 100 million of MRI scans are conducted, with an estimated fractions of scans between 30% to 45% that involves the administration of GBCAs. (Scarciglia et al., 2025) Averaging a dose of

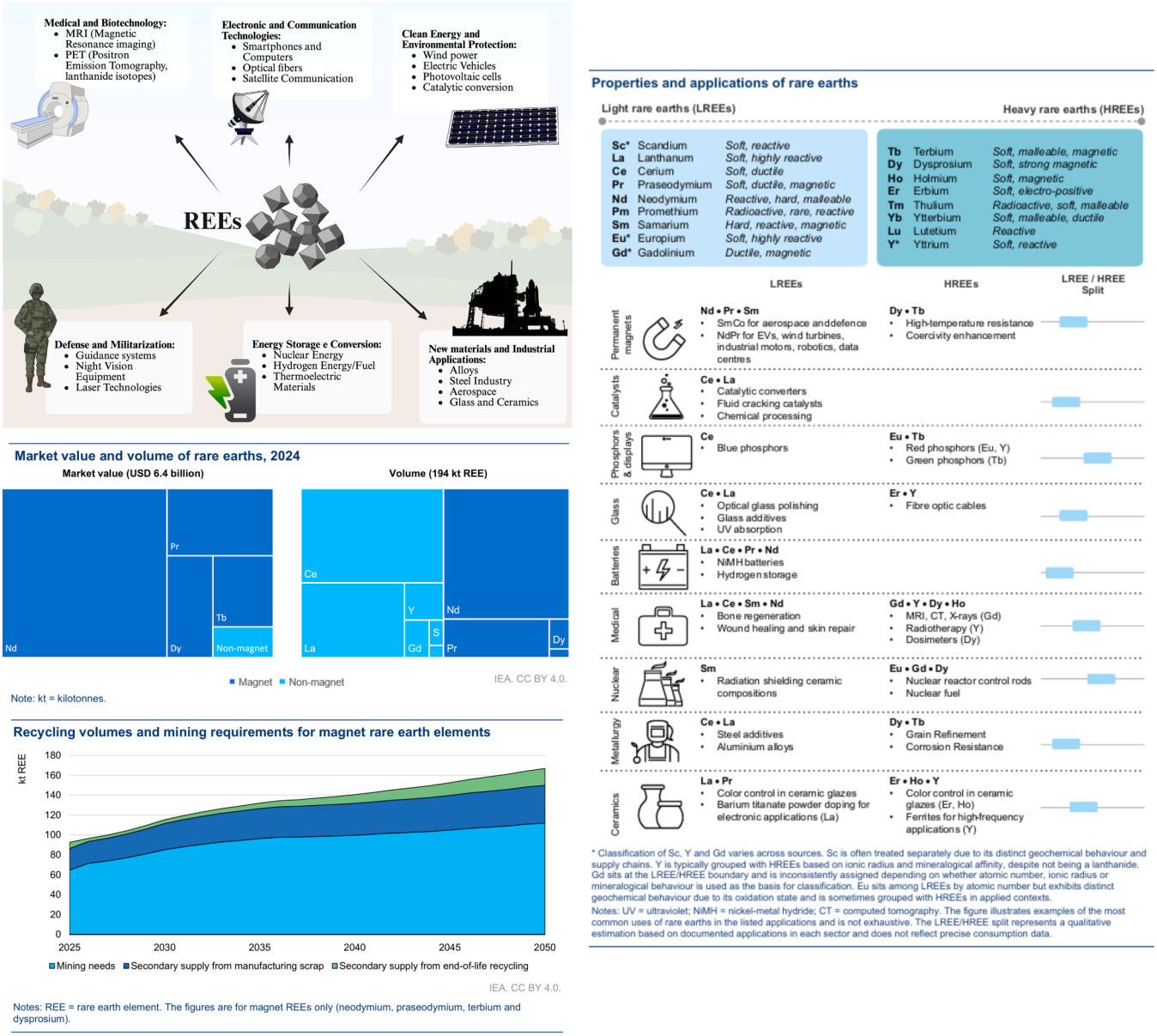


Fig. 1. Applications and impact of rare earth elements (REEs) on global economy. This is a work derived by Scarciglia et al from IEA material and Scarciglia et al are solely liable and responsible for this derived work. The derived work is not endorsed by the IEA or its Member countries in any manner (International Energy Agency (IEA) 2026).

Gd^{3+} per scan of 0.8g to 1.5g, a total amount of gadolinium excreted and released in wastewater could be estimated in 35 to 55 tonnes. However, in the specific case study discussed here, solutions to be treated will be enriched in GBCAs, for this reason a double approach could be considered, as from one side complexes could be captured as shown by Wijesinghe, S. et al (Wijesinghe et al., 2026), an alternative decomplexation pretreatment step could be conducted before the sorption process, to obtain free Gd^{3+} ions. While linear GBCAs such as Gd-BOPTA are susceptible to UV photolysis, macrocyclic GBCAs like Gd-DOTA exhibit significantly higher kinetic stability (Birka et al., 2016). Advanced oxidation processes (AOPs) employing hydroxyl radicals (•OH) have shown promise for weakening both linear and macrocyclic GBCAs (Cyris et al., 2013). Cyris et al. demonstrated that •OH radicals, generated through O_3/H_2O_2 or O_3/UV systems, react with GBCAs at near-diffusion-controlled rates ($k \approx 10^9\ M^{-1}s^{-1}$). The oxidative attack fragments the organic chelating ligands, producing less stable Gd-complexes that can more readily dissociate under mildly acidic conditions. Indeed, recent studies have demonstrated that even untreated macrocyclic GBCAs can be degraded under sufficiently acidic conditions. Gd-DOTA, for example, showed dissociation half-lives of approximately 14 days at pH 1 and 25°C, with up to 29% degradation observed after 5 weeks at pH 2 (Guerreiro and Brito, 2023, Idée et al., 2009). Even if such an integrated approach falls outside the scope of the present study, a combined approach involving AOP pretreatment followed by acidification would facilitate the release of free Gd^{3+} ions suitable for subsequent recovery by sorbents, and must be considered for future research.

The approach presented herein introduces natural minerals as adsorbents for the selective capture of REEs from aqueous solutions through a simple solid–liquid extraction (SLE) strategy (Elgoud et al., 2022). Their natural availability and minimal processing requirements may offer advantages over more complex engineered sorbents. Several materials are investigated in the field of metal recovery and decontamination, such as synthetic adsorbents (Martínez-Montoya et al., 2024, Marchesi et al., 2020, Gupta et al., 2021), commercial activated carbon (Mariana et al., 2021, Michałek et al., 2025, Qiu et al., 2022) synthetic zeolites and layered materials (Mosai et al., 2019, Hong et al., 2019, Zhang et al., 2025), engineered sponges (Zhang et al., 2025, Morton et al., 2025) and membranes (Abdullah et al., 2019, Edward et al., 2024), which, although effective in removing contaminants, require more sophisticated techniques and higher processing costs (Awual et al., 2023, Waliullah et al., 2023). The dioptase cyclosilicate ($Cu_6Si_6O_{18}$), consisting of interconnected Si_6O_6 rings (Reddy et al., 1986), is commonly recognized as a pigment, but the powder generated by the ball mill process could be considered for further applications, such as those in the environmental protection field. We started our investigation with a structural, morphological and spectroscopic analysis of the cyclosilicate, then we studied its ability to capture lanthanides metals as gadolinium (Gd^{3+}), lanthanum (La^{3+}) and lutetium (Lu^{3+}) from aqueous solutions, under different experimental conditions, focusing on the adsorption mechanism and kinetics.

An intermediate concentration of 0.1 mM was selected to investigate the adsorption mechanism, kinetics, and regeneration of the sorbent under well-controlled laboratory conditions. This concentration does not aim to reproduce a specific environmental or clinical scenario but provides a practical model system for mechanistic investigations. The applicability of the proposed approach to real GBCA-containing wastewater will require a preliminary decomplexation step and validation in real matrices. This proof-of-concept approach establishes the experimental basis for future validation under more complex and realistic wastewater conditions.

The capture process of paramagnetic Gd^{3+} was monitored by ^{1}H-NMR relaxometry (Marchesi et al., 2022, Werner et al., 2022), and the quantitative data were confirmed by inductively coupled plasma mass spectrometry (ICP-MS). The use of low resolution ^{1}H-NMR relaxometry makes possible to monitor the relaxation times (T_1 and T_2) of water protons in solution. Since lanthanides are paramagnetic relaxation agents, they shorten water proton relaxation times, so their depletion from solution causes measurable relaxation time lengthening that directly correlates with adsorption extent (Ancora et al., 2024, Gossuin and Vuong, 2018). This approach is useful as it also enables real-time, non-invasive tracking, of the adsorption kinetics for single or multiple lanthanides simultaneously, in a single experiment, revealing differences in their binding mechanisms and affinities toward the cyclosilicate without requiring sample separation or destruction. Finally, desorption tests were carried out for metal recovery and possible regeneration of the sorbent material. To the best of our knowledge, this study represents the first systematic investigation of this natural cyclosilicate for metal removal applications, with a promising balance between performance, sustainability, and economic viability.

Materials and methods

Dioptase ($Cu_6Si_6O_{18}\cdot 6H_2O$) was purchased from Kremer Pigmente (Germany). Gadolinium(III) chloride ($GdCl_3$), lanthanum(III) chloride ($LaCl_3$), lutetium(III) chloride ($LuCl_3$), sodium chloride (NaCl), boric acid (H_3BO_3), hydrofluoric acid (HF), hydrochloric acid (HCl), nitric acid (HNO_3), and barium sulfate ($BaSO_4$) were obtained from Sigma-Aldrich/Merck and used without further purification. Gadoteridol (Gd-HPDO3A, ProHance; Bracco Imaging) was used as reference compound. All solutions were prepared with ultrapure water and filtered through 0.2 µm syringe filters. pH was adjusted and monitored using standard buffer calibration.

Characterization methods

Phase composition was evaluated by powder X-ray diffraction (XRPD, Bruker D8 Advance Powder Diffractometer). Morphology was examined by field-emission scanning electron microscopy (GeminiSEM 360 Zeiss equipped with Schottky-type field emission electron gun) after conductive coating (Sputter-Coater EMITECH K575). Optical properties were assessed by diffuse reflectance UV–Vis spectroscopy using $BaSO_4$-diluted samples (Perkin Elmer Lambda 900 Spectrophotometer). Mineralogical changes after adsorption were verified by comparing pre- and post-treatment samples.

Adsorption procedure

Adsorption experiments were performed in batch mode using polypropylene tubes under continuous orbital agitation to ensure suspension of dioptase particles at a fixed sorbent-to-metal mass ratio. Aqueous solutions of $GdCl_3$, $LaCl_3$, and $LuCl_3$ (0.1 mM) were prepared at pH 5.5 to prevent metal hydrolysis. In the all experiments, at fixed time intervals (24 hours, considered as the end of each cycle), the solution was recovered, filtered and replaced with the same volume of an untreated solution, while the treated ones were processed for ^{1}H-NMR and/or ICP quantification, and subsequently stored at 4°C. All experiments were conducted in at least duplicate. Additional tests were performed at pH 2.0 to evaluate stability under acidic conditions. Competitive adsorption experiments were carried out by exposing pre-loaded dioptase to single- and mixed-metal solutions (Na^+, La^{3+}, Lu^{3+}). After each cycle, washing steps were applied to remove unbound ions prior to further exposure.

Quantification of $Gd^{3\pm}$ concentration

Residual Gd^{3+} concentration in solution was determined by ^{1}H NMR relaxometry and validated by ICP-MS. Samples were acidified (HCl 37%) prior to analysis to ensure complete dissolution of any residual species. R_1 of each solution was measured at 21 MHz and 298 K, using a Stelar SpinMaster Relaxometer (Mede, Pavia, Italy). The paramagnetic metal concentration was calculated by applying the following equation (Eq. 1):

$$[Gd^{3+}] = \frac{R_1 - R_d}{r_{1p}} \quad \text{(Eq. 1)}$$

where R_1 is the ^{1}H longitudinal relaxation rate, R_d is the longitudinal relaxation rate observed for the blank and, finally, r_{1p} is the relaxivity of the paramagnetic solution.

Mass-weighted distribution coefficient

The adsorption efficiency was expressed as the mass-weighted distribution coefficient (K_d, mL g^{-1}) (Eq. 2):

$$Kd = \left(\frac{(C_i - C_f)}{C_f}\right) \times \left(\frac{V}{m}\right) \quad \text{(Eq. 2)}$$

where C_i (mM) is the initial concentration of the metal, C_f (mM) is the concentration of the metal after equilibrium has been reached, V (mL) is the solution volume, and m (g) is the sorbent mass.

Mathematical modelling of $Gd^{3\pm}$capture kinetics

Adsorption kinetics were evaluated using standard kinetic models including zero-order, first-order, Bhaskar, parabolic diffusion, and modified Freundlich models applied to experimental ^{1}H NMR relaxometric data. A complete description and physical meaning of each of these models are detailed in the study of Zhang *et al.* (Zhang et al., 2009). The best fit was obtained using a diffusion-controlled parabolic model indicated as Eq. 3:

$$1 - \frac{\frac{M_t}{M_0}}{t} = -k_p t^{-0.5} + m \quad \text{(Eq. 3)}$$

where M_0 and M_t are the concentrations (mM) of paramagnetic ion at the beginning of the tests and at various contact times t, k is the kinetic constant of the uptake process and m is a constant.

Acid mineralization procedure of dioptase powders and metal solutions for metal quantification

For total metal quantification, dioptase samples were digested using HF and aqua regia under microwave-assisted conditions. Liquid samples were acidified and prepared for analysis by freeze-drying and redissolution in nitric acid when required. Metal concentrations (Gd, La, Lu, Cu) were determined by ICP-MS and ICP-OES using external calibration with certified standards (Thermo Scientific ELEMENT 2 ICP-MS-Finnigan and Perkin Elmer, Norwalk, CT, USA, ICP-OES).

Experimental setting for uptake tests

In detail aqueous specimens containing 0.1 mM of Gd^{3+} at mildly acidic (pH 5.5) (Step 1, Scheme 1), were mixed with dioptase powder in specific stoichiometric ratios in plastic test tubes (Step 2, Scheme 1), under gentle agitation for 24 h in an orbital shaker (Step 3, Scheme 1), the filtered solutions were then analyzed for metal quantification (Step 4a,b, Scheme 1). The dioptase powder was then re-used for subsequent uptake cycles (Step 5, Scheme 1). Finally, the amount of Gd^{3+} removed by was measured (Step 6, Scheme 1).

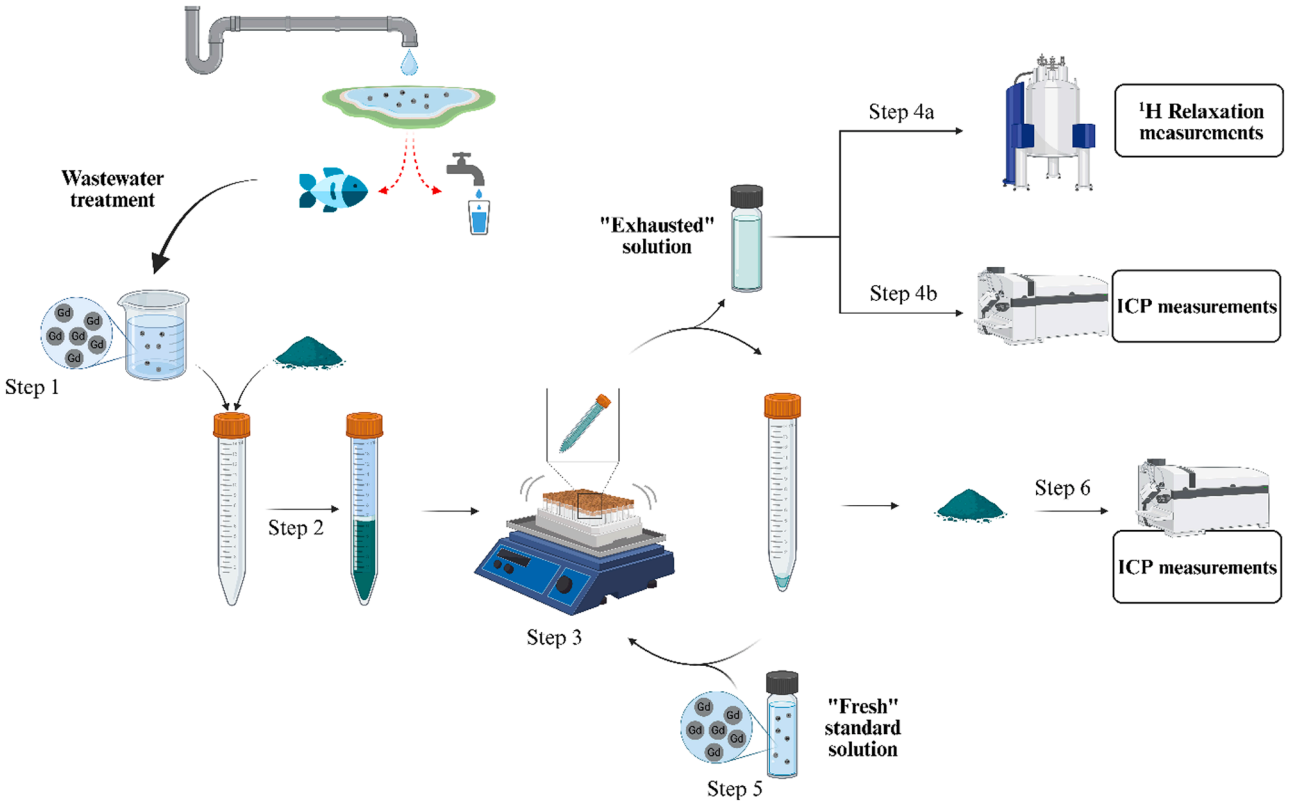
Software and tools

Data processing and visualization were performed using OriginPro. Mineral phase identification was carried out using DIFFRAC.EVA. Structural visualization was performed using VESTA. Fig.s were prepared using BioRender.

Results

Structural and morphological analysis of dioptase

Dioptase, a natural hydrated copper cyclosilicate mineral



Scheme 1. Experimental set-up considered for testing metal removal from aqueous solution by using dioptase powder.

($Cu_6Si_6O_{18}·6H_2O$), was investigated as a potential sorbent for lanthanide ions in aqueous solutions. Its unique crystal structure, characterized by isolated hexagonal rings of silica tetrahedra (Si_6O_{18}) (Kumasaka et al., 2024-, interconnected by Cu^{2+} ions, and channels that can facilitate the ion exchange process, along with its surface composition rich in hydroxyl groups, makes it a promising candidate for selective adsorption processes (Fig. 2A). The structure analysis of dioptase was carried out by X-ray powder diffraction technique (PXRD) before and after the uptake tests, as a result the stability under ion-exchange conditions indicated that adsorption does not induce bulk framework collapse, which is critical for long-term recyclability (Fig. 2B). Before uptake tests the profile shows the crystallographic reflections typical of the dioptase structure, in accordance with the X-ray patterns reported in the PDF-2 2004 card no. 033-0487 (Fig. S1) of the hydrated copper silicate and ICDD card no. 33-487 (Law et al., 2010, Mindat, 2026). The X-ray diffraction profile suggests the presence of the typical trigonal-rhombohedral crystal structure (space group R) of the dioptase mineral (Colombo et al., 2012, A refinement of the structure of dioptase). X-ray diffractograms of dioptase after saturation test with Gd^{3+} ions, after subsequent cation-exchange with La^{3+} ions and after regeneration in acidic conditions (pH 2 and 6) are also reported in Fig. 2B. The overall structural features of dioptase are well preserved after each test, with no significant modifications in the position and/or intensity ratio of the signals, thus indicating a high chemical stability of the inorganic architecture without alteration of the crystal structure. The morphological analysis of the dioptase was carried out by using field emission scanning electron microscopy (FE-SEM), and the results are shown in Fig. 2C and Fig. S1. FE-SEM micrographs of dioptase reveal a prismatic-like morphology with an irregular spatial organization of particles, with a surface characterized by microfractures and roughness. Dioptase, despite its trigonal-rhombohedral crystal system, very frequently grows as elongated six-sided prismatic crystals. These prisms often terminate with the characteristic three faces of a rhombohedron (or, sometimes, scalenohedral faces): thus, while the underlying symmetry is 3-fold rotational, the crystal growth often favors elongation along that unique 3-fold axis, resulting in a prismatic habit (Colombo et al., 2012). At low magnification (Fig. S1A), the cyclosilicate appears as an aggregate of fragmented crystals with sharp edges. At higher magnifications (Fig. 2C and S1), elongated prismatic crystals can be observed, deposited mainly on the surface of the aggregated particles, with crystal surfaces showing a degree of granularity and irregularity, with jagged edges indicative of either imperfect euhedral growth or post-crystallization breakage.

Diffuse reflectance (DR) UV-Visible spectrum of dioptase shows the presence of two high-energy bands located at 262 and 305 nm, and a broad band centered at *ca.* 760 nm (Fig. 2D). The first two signals can be attributed to ligand-to-metal charge-transfer (LMCT) electron transitions from oxygen groups in SiO_4^{4-} units to the structural Cu^{2+} ions, while the broad band at low energy can be assigned to *d-d* electronic transitions of the Cu^{2+} ion in distorted octahedral geometry. As shown in the graphical representation of the structure of dioptase of Fig. 2A, each Cu^{2+} ion is bonded to four distinct structural oxygen atoms within various silicates and to two elongated axial water molecules (Ament et al., 2011, Li et al., 2012, Chmielarz et al., 2006).

Uptake tests

The experimental setup adopted in this work, as reported in Scheme 1, was designed to investigate the adsorption behaviour of dioptase toward free lanthanide ions under controlled laboratory conditions and to

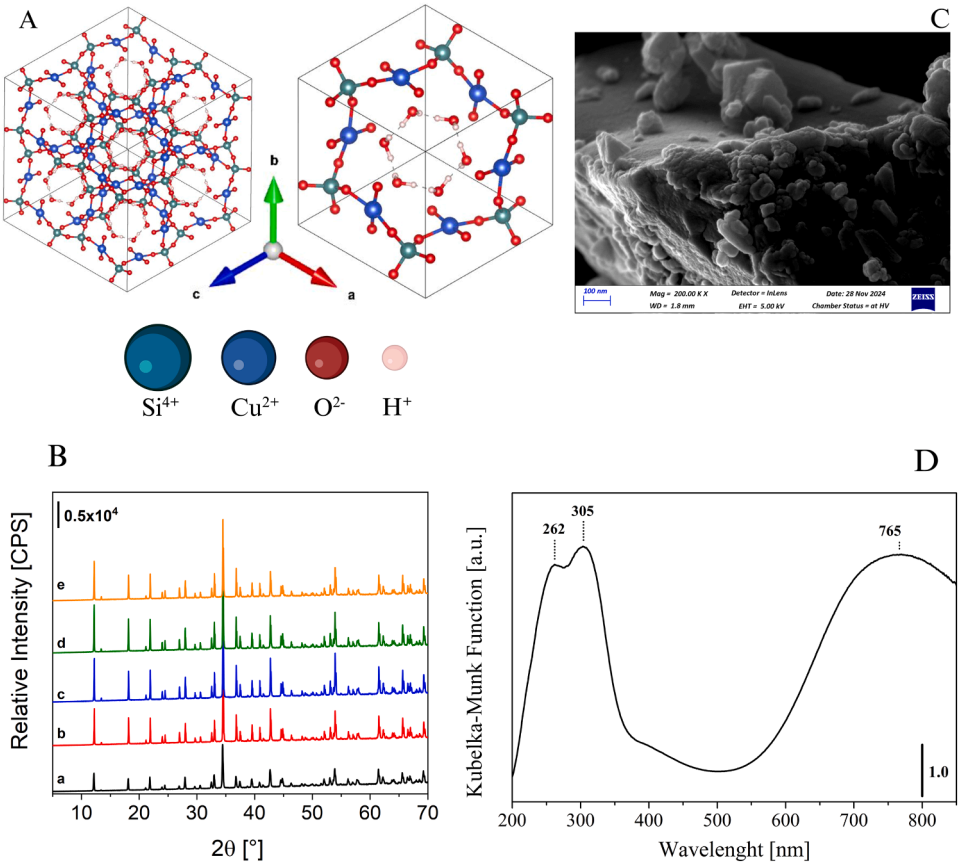


Fig. 2. A) Graphical representation of the dioptase crystal structure projected on the [101] crystallographic direction on the left and [111] on the right, obtained by VESTA software. B) X-ray profiles of dioptase before (a) and after saturation with Gd^{3+} (b), cation-exchange with La^{3+} (c) and regeneration at pH 2 (d) and 6 (e). C) FE-SEM micrograph of dioptase at high magnifications. D) Diffuse Reflectance (DR) UV-Visible spectrum of dioptase, collected in vacuum at room temperature.

evaluate its potential as a natural sorbent. For this reason, the following experiments have been carried out at a fixed concentration of 0.1 mM of Gd^{3+} ions in water solutions.

Initially, we evaluated the adsorption capacity of dioptase for Gd^{3+}, in form of free ions, or as GBCA (herein we used Gadoteridol), in different weight ratios between sorbent and metal over 24 hours. We considered three different mass ratios (mass:mass) of dioptase/Gd^{3+}, fixed to 20:1, 1000:1 and 5000:1.

Fig. 3 shows the R_1 values of water protons of the filtered supernatants of tested Gd^{3+}-contaminated aqueous solutions (as ions of chelates) after 24h of contact with the sorbent powder at 0.5 T and 298 K. No significant uptake of the macrocyclic GBCA (ProHance) occurred over time (Fig. 3a), unlike what can be observed in the case of the Gd^{3+} ions solution (Fig. 3b), with a reduction of R_1 of approximately 100% at the highest mass ratios (%) of dioptase/Gd^3. These results indicate that the method in its current form is not applicable to intact GBCAs containing matrices, but to free lanthanide ions, requiring a prior decomplexation step.

R_1 of pure dioptase in water is also reported for reference (Fig. 3c), showing a constant R_1 value which indicates no significant release of paramagnetic species -from the powder- that could affect the measures. By testing solutions containing $GdCl_3$, a decrease of R_1 has been observed (Fig. 3 b), exponentially proportional to the amount of dioptase present (*i.e.* from 1.17 ± 0.01 s^{-1} in absence of dioptase to 0.95 ± 0.01 s^{-1}, 0.72 ± 0.01 s^{-1} and 0.49 ± 0.02 s^{-1} in presence of an excess of 20, 1000, 5000 mass ratios of dioptase/Gd^{3+}, respectively). When the mass ratio dioptase/Gd^{3+} is 5000, the R_1 reaches the value of blank (0.48 ± 0.01 s^{-1}, Fig. 3c), indicating that all Gd^{3+} ions originally present in solution have been removed, hence we selected this condition as the reference one for any other capturing test.

Afterwards, we monitored under real-time condition Gd^{3+}-uptake over 24 h. In detail, dioptase (9.45 mg) was added at the bottom of 5 mm NMR glass tubes and 120 μL of an aqueous 0.1 mM $GdCl_3$ solution at pH 5.5 was carefully added, keeping the selected dioptase/Gd^{3+} mass ratio of 5000. The selected pH (5.5) represents the optimal compromise between metal solubility and adsorption performance. Measurements of longitudinal relaxation times R_1 were carried out immediately after adding the metal solution, at 0.5 T and 298 K. The concentration of gadolinium species in solution after contact with dioptase was then determined by Eq. 1 (Marchesi et al., 2020). As shown in Fig. 4 the R_1 (herein normalized to 100%) decreases rapidly, reaching a -50% of the initial value at approx. 3 h of contact with the substrate, with a final *plateau* after 5 h. After 7 h, 99.6% of the metal content was removed by dioptase. Using Eq. 1, we extrapolated the amount of sequestered Gd^{3+} over time (mmol of Gd^{3+} per g of dioptase) (Fig. 4C). After 24 hours, the measured R_1 value corresponds to that of water in the presence of dioptase alone (diamagnetic contribution), suggesting a complete removal of the Gd^{3+} ions from the aqueous solution.

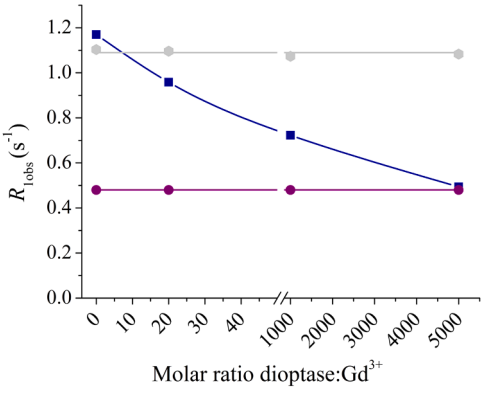


Fig. 3. Uptake of (a) Gd^{3+} and (b) ProHance with different mass ratio dioptase/Gd^{3+}. (c) R_{1obs} for dioptase in water. At the selected time point of 24 hours, samples are centrifuged, supernatants containing non adsorbed gadolinium ions/chelates were recovered and filtered using 0.2μm cellulose filter.

An assessment on the kinetics of Gd^{3+} uptake process by dioptase was performed with the results shown in Fig. 4. The process was quantitatively analyzed with several mathematical models (zero-order model, first-order model, Bhaskar Equation, parabolic diffusion model and a modified Freundlich model (Zhang et al., 2009)) in order to obtain more insights on the sequestration mechanism (Zhang et al., 2019, A refinement of the structure of dioptase, 2021, Sen Gupta and Bhattacharyya, 2011, Raji et al., 2023). Among all models tested, the one that best fits our experimental data is the parabolic diffusion pattern (Fig. 5), which describes a metal removal mechanism mainly governed by diffusive phenomena (Awual et al., 2019, Shahat et al., 2021). The kinetic constant, calculated by analyzing the NMR relaxometric data with the parabolic model, was found to be 0.54 s^{-1}, with the highest correlation coefficient (R^2) among all models tested, equal to 0.9885. After the first cycle, a mass-weighted distribution coefficient (K_d) of 641.3 mL g^{-1} ($\log K_d = 2.81$) was calculated by applying Eq. 2. Based on these results, contact time optimization was obtained, as we can confirm that a dioptase/Gd^{3+} mass ratio of 5000 is sufficient to completely remove all Gd^{3+} from a 0.1 mM solution when the contact time exceeds 7 hours. Subsequently, the ability of dioptase to remove Gd^{3+} from aqueous solution in multiple uptake cycles was explored. For this purpose, we repeated the capture experiment for several cycles to understand the loading capacity of the sorbent. The test was conducted for 8 cycles, keeping the same experimental condition over 24 hours *per* cycle (298 K and the 5000:1 dioptase:Gd^{3+} mass ratio) (Fig. 6). The residual concentration of the metal in the treated solution was monitored by ^1H NMR relaxometry at 0.5 T and 298 K (Fig. S3) and the quantification of Gd^{3+} sequestered *per* g of sorbent is reported in Fig. 6A. The ability of dioptase to adsorb Gd^{3+} decreases progressively with successive cycles of sorbent reuse. After the first one, in which complete removal of gadolinium was achieved, an overall reduction in capture efficiency is observed in the remaining cycles (in particular from the 3rd cycle), reaching a removal capacity of approx. 23% of the Gd^{3+} content available in solution after the 7th cycle. At the end of the test, the total amount of Gd^{3+} captured by dioptase was calculated to be (5.25 ± 0.07) × 10^{-3} mmol g^{-1}. To validate the relaxometric measurements and confirm the structural integrity of dioptase during the adsorption process, ICP-MS analysis was performed on selected aqueous supernatants collected (Fig. 6B). Three representative supernatants, corresponding to the first, a middle, and final cycles, were analyzed to quantify Gd^{3+} and Cu^{2+} concentrations, confirming relaxometric observations. In the first cycle, negligible Gd^{3+} was detected in the supernatant, indicating near-complete adsorption by the mineral while in the middle cycle, the Gd^{3+} concentration in solution increased, reflecting the reduced availability of binding sites and incomplete adsorption. By the final cycle, the Gd^{3+} concentration in the supernatant increased further, consistent with the diminished sorption capacity observed in the R_{1obs} measurements. Importantly, no significant Cu^{2+} amount was detected in any of the supernatants throughout the loading cycles, confirming that the dioptase structure remained intact with no leaching of structural copper from the mineral matrix during the adsorption process. This agreement between relaxometric and ICP-MS data validates the use of NMR relaxometry for monitoring lanthanide adsorption on mineral surfaces.

To evaluate the practical applicability of dioptase for Gd^{3+} recovery and potential reusability, we investigated the stability of both unloaded and Gd^{3+}-loaded dioptase under different aqueous conditions. No significant release of Cu^{2+} ions -from dioptase- into the solution was observed during the cycles, indicating that the experimental R_1 values are attributable exclusively to the gadolinium content in water (Fig. 6B, Fig. S6). As reported in Fig. 7A, no significant increase in R_{1obs} was observed, indicating no detectable release of paramagnetic species, confirming structural integrity of the mineral and at the same time the retention of the metal for the Gd^{3+}-loaded powder, with no release of Cu^{2+} or Gd^{3+} ions over 6 cycle steps in pure water and pH 5.5 (Fig. S5,

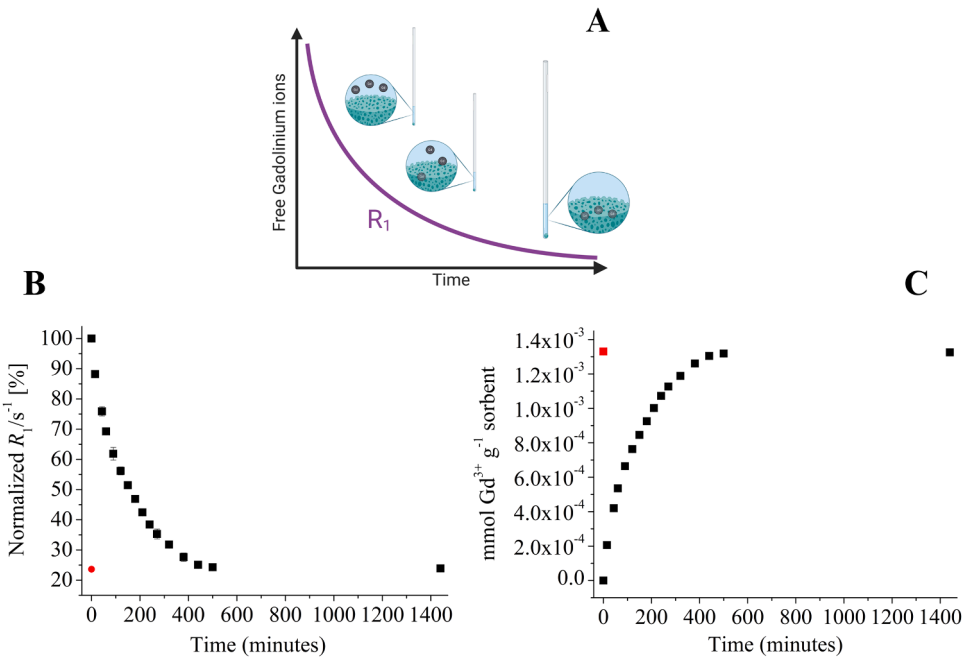


Fig. 4. First cycle of removal, points acquired during the first 24 hours. A) Schematic representation of metal adsorption and R_{1obs} behavior. B) Decreasing in the free Gd^{3+} in solution represented as a decreasing signal (R_1) over time, in red the signal for pure water. C) mmol of Gd^{3+} adsorbed *per* g of dioptase over time; in red the mmol of a 0.1 mM Gd^{3+} solution.

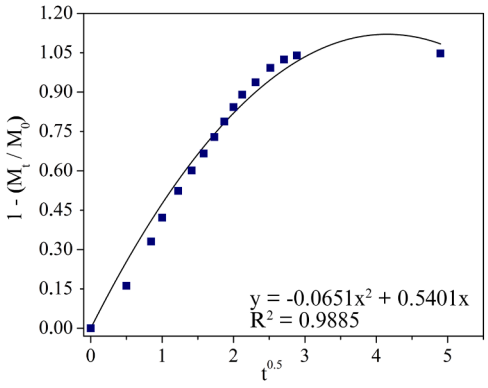


Fig. 5. Kinetic analysis of the Gd^{3+} removal data for dioptase in the first cycle of uptake shown in the Fig. 4.

S6).

Quantification of Gd^{3+} and Cu^{2+} by ICP-MS analyses was also performed on the samples to further confirm these data (Fig. S2). The stability of the silicate structure and the retention of the Gd^{3+} was further confirmed in the presence of high ionic strength, by treating dioptase with a saturated NaCl solution (Fig. 7B). For the experiment being conducted on Gd^{3+}-saturated dioptase, after 8 treatment cycles, the powder was first washed to remove any non-adsorbed gadolinium, freeze dried, and then re-suspended in a NaCl solution. Then, 6 uptake cycles (24 hours each) were performed on the metal-loaded powder, using an orbital shaker for the agitation of the system. At the end of each cycle, the supernatant was removed by centrifugation and replaced with a fresh NaCl solution. The modified sorbent appeared to be stable under the tested condition, as no significant release of Gd^{3+} from the Gd^{3+}-loaded silicate was observed, as shown in Fig. 7B.

Following the previous experiments, the regeneration capability of dioptase in the context of sustainability and recycling of the inorganic matrix in a real-world application was assessed. To this end, dioptase was brought in contact with strongly acidic solutions after Gd^{3+}-uptake. As a reference value, commercial cyclosilicate was placed in an acidic aqueous solution at pH 2 and 298 K in an orbital shaker and tested in 6 cycles. In each one, the supernatant was removed and replaced with fresh acidic water, with the pH controlled and kept constant throughout all cycles.

As shown in Fig. 8A, treatment of dioptase at pH 2 causes a partial increase of the R_{1obs} value for the supernatant, indicating a release of paramagnetic metals in solution. After the saturation steps, the Gd^{3+}-loaded powder was considered for the same experimental setting at pH 2 (Fig. 8A). As shown, the variation between the two curves appears to be more relevant in the first three cycles, and the increase in the R_1 value was due to the strong release of Gd^{3+} in solution. The Gd^{3+} released after the acidic treatment was calculated to be close to 95% in moles respect to the total amount captured in the previous 7 adsorption cycles, as they are calculated to be $(4.31 \pm 0.05) \times 10^{-3}$ mmol g^{-1}, showing a near-complete release of the metal. Data reported in Fig. 8B and Fig. S5 acquired via ICP-MS confirmed the behavior. As reported in Fig. 2B and Fig. S6, XRD analysis confirms no structural damages or changes after treatment with acidic condition, meaning that the phenomenon reported depends on non-structural Cu^{2+} release during the cycles. We then decided to evaluate if pre-conditioning in acidic condition of the powder could affect the adsorption capacity of the silicate. As reported in Fig. 8C after six days of acidic treatment (pH 2) in which an increase in the R_1 value is reported, due to paramagnetic metal species release, the powder was put in contact with a 0.1 mM gadolinium solution, and 6 saturation steps were conducted. In this case, no significant decrease in the R_1 value was observed, which is indicative of a poorer capturing capacity, meaning no significant amount of Gd^{3+} was removed from the solution. Excluding any structural damage, these results are probably due to the competition of H_3O^+ delocalized in the channels of the adsorbent with the metal cations.

The affinity of the sorbent for other lanthanides was also explored, selecting lanthanum (La^{3+}) and lutetium (Lu^{3+}) to evaluate any size/charge affinity mechanism during the experiments (Islam et al., 2025, Zhang et al., 2025). These two lanthanides display specific coordination numbers and ionic radii (for CN = 6 the ionic radii are La^{3+}:1.027 Å > Gd^{3+}:0,929 > Lu^{3+}:0.831. Data reported in Table S1, Fig. S7), as a

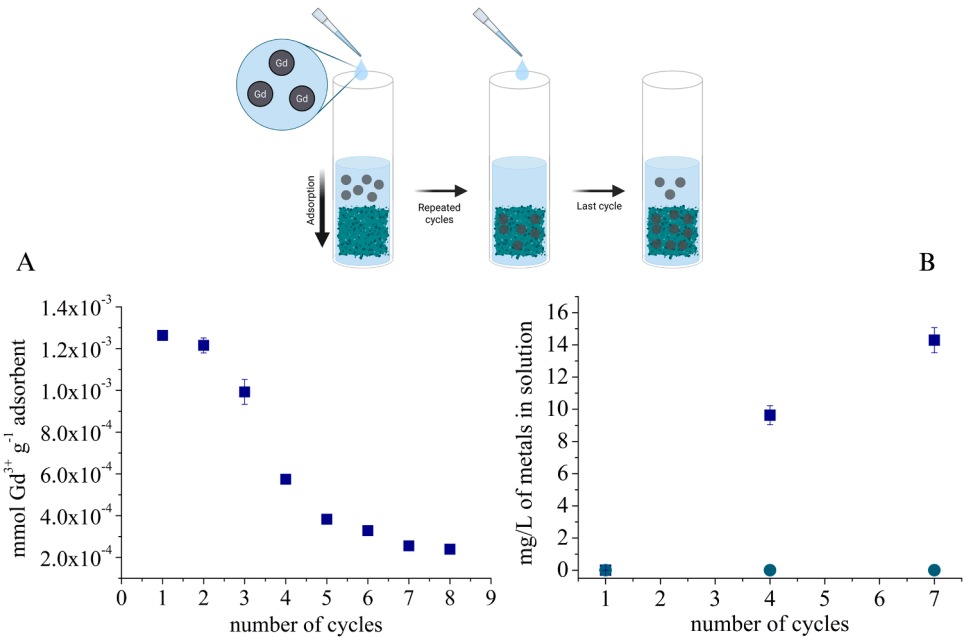


Fig. 6. A) mmol of Gd^{3+} adsorbed per g of sorbent per cycle. B) ICP-MS analysis of solutions to test for Cu^{2+} (green dots) and Gd^{3+} (blue dots), gadolinium signal increases as sorption capacity decreases in the last cycles.

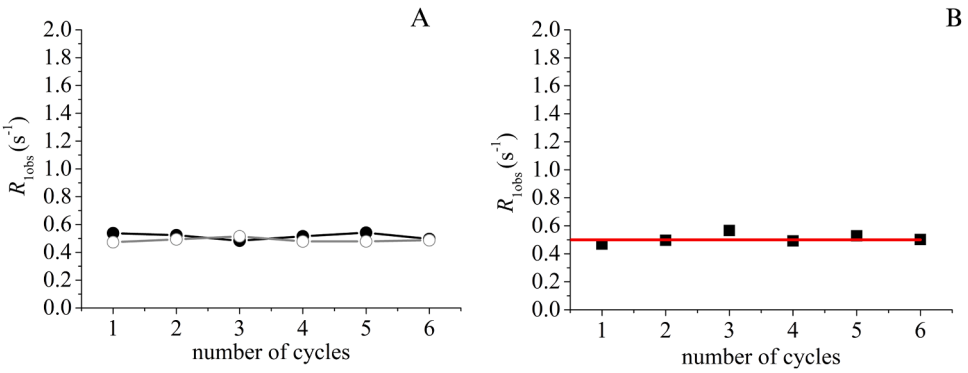


Fig. 7. A) commercial powder tested over 6 cycles as source of paramagnetic contribution, to distinguish between intrinsic paramagnetism (grey line for commercial dioptase) and potential Gd^{3+} release from Gd^{3+}-loaded dioptase (pH = 5.5, black line). B) stability of adsorbed Gd^{3+} in the presence of a saturated NaCl water solution (black dots, red line as the reference NaCl solution R_{1obs} value). For each condition, no significant increase in R_{1obs} observed.

consequence of the lanthanide contraction phenomenon (Lundberg et al., 2010, D'Angelo et al., 2011).

To this end, we first treated two independent batches of the dioptase with a 0.1 mM Gd^{3+} solution. At the end of six loading cycles, for both of the two independent Gd^{3+} loaded matrices, we quantified the amount Gd^{3+} adsorbed. Powders were then washed to remove any non-adsorbed Gd^{3+} ion. Subsequently, a solution containing an excess of La^{3+} or Lu^{3+} ions with respect to Gd^{3+} in the uptake solutions (molar ratio of 20:1) was prepared to perform lanthanide exchange tests, aimed at evaluating the efficiency/selectivity of lanthanide substitution, on the previously mentioned loaded matrices. In the substitution test, fresh La^{3+} or Lu^{3+}solution was added for 6 cycles to the corresponding sorbent batch, while the removed exhausted supernatant at the end of each cycle, was processed for relaxometric quantification of the gadolinium released. In addition, in low-field NMR relaxometry (0.5 T), the observed signal arises from the longitudinal (T_1) and transverse (T_2) relaxation of nuclear spins. Paramagnetic ions such as Gd^{3+} enable the exploitation of dipolar interactions with surrounding water protons. In contrast, La^{3+}, being diamagnetic, and Lu^{3+}, with negligible unpaired electron density, do not significantly affect proton relaxation. Therefore, any observed variation in relaxation can be attributed solely to the presence of a varying Gd^{3+} concentration.

Comparing the results for both the considered lanthanides, Lu^{3+} treatment (Fig. 9B) leads to a sharper and more pronounced initial release of Gd^{3+} (Fig. 9C), suggesting a stronger competitive displacement effect, with the majority of Gd^{3+} released in the first two cycles in both the experiments, indicating that a significant fraction of the adsorbed Gd^{3+} is readily exchangeable under the applied conditions. In contrast, the desorption profile of the La^{3+}-treated system shows a more gradual decrease (Fig. 9 A, C, Fig. S4), with residual Gd^{3+} continuing to be released over several cycles with a behavior indicating a less efficient exchange process in the presence of La^{3+}, possibly due to weaker interactions with the sorbent or lower competitiveness in occupying the interaction sites. Looking in detail, the moles of gadolinium released after the treatment with the other lanthanides (Fig. 9D), the moles released in the presence of Lu^{3+} where 89.91 ± 2.86 % from the total Gd^{3+} captured, compared to the 61.38 ± 1.40 % value of La^{3+}, confirming the hypothesis.

To gain insight into the underlying adsorption mechanism, the process was investigated in the simultaneous presence of different

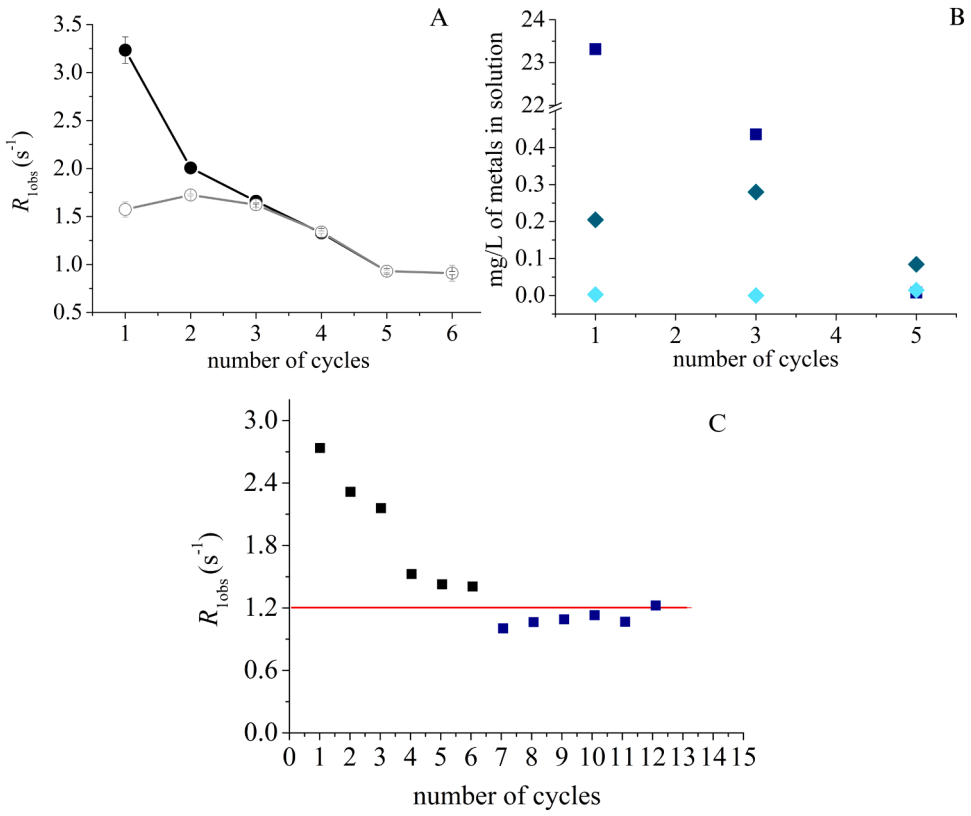


Fig. 8. A) Testing of metal desorption under acidic conditions (pH = 2), grey line shows commercial dioptase signal over 6 cycles, black line shows Gd^{3+}-loaded powder under acidic conditions. The difference between the two curves correspond to the Gd^{3+} released in the tested conditions. B) ICP-MS analysis of the same solutions to test for Cu^{2+} and Gd^{3+} release. In blue gadolinium signal decreases over the testes cycles, confirming the relaxometric data as the amount of desorbed metal decreases over time. In green the signal from Cu^{2+} released (at pH = 2) compared to the Cu^{2+} signal at pH = 5 (light blue). C) pre-conditioning of the powder, black dots are referred to the 6 days of acidic treatment of the sorbent, this treated dioptase was then considered for Gd^{3+} adsorption (blue dots) showing no variation as no Gd^{3+} captured, the red line represents the standard Gd^{3+} 0.1 mM solution signal.

lanthanides (Awual et al., 2017) Lu^{3+} being the smallest trivalent lanthanide, has a higher charge density than Gd^{3+} and La^{3+}, and this leads to a greater electrostatic attraction and a more favorable inner-sphere complexation with the surface of dioptase at pH 5.5 compared to the other two metal ions (Jordan et al., 2010). It is known that the number of water molecules in the first coordination shell in the lanthanide series decreases across the series, as La^{3+} has a larger first hydration shell compared to smaller lanthanide ions as we move from a CN of 9 to 8 along the series (Miller et al., 2017, Rudolph and Irmer, 2020), and this could impact the interaction with silica surface. Considering radius size, smaller ions with the most exothermic hydration free energy (ΔG_{hydr}), with a difference between La and Lu in water amounting to 416 kJ mol^{-1} (Sijl, 2011, D'Angelo and Spezia, 2012), could easier bind to external sites or diffuse and bind more in internal sorbent sites (Tansel et al., 2006, Ogata and Narita, 2024). Lu^{3+} is able to 'approach' silica surfaces more closely due to the preferential inner sphere coordination, this leads to a more efficient adsorption and of a favorable displacement of previously adsorbed Gd^{3+} ions (Ilgen et al., 2023). Considering La^{3+} tendency to form weaker outer-sphere complexes, it seems to be less 'reactive' toward the silica surface and less effective at displacing Gd^{3+} ions already adsorbed on them.

Lastly, a competition test was carried out with all the three metal ions simultaneously present in the test solution. As shown in Fig. 10, the adsorption tests were conducted for 9 cycles.

The concentration of each metal in the solution was fixed to 0.1 mM for each metal Gd^{3+}, La^{3+} and Lu^{3+}. As previously described, at each step the solution was completely removed and processed for subsequent quantitative analysis and substituted with the standard solution of the three metals. As reported in Fig. 10, Lu^{3+} exhibited a greater uptake compared to the other metals, showing at the end of the cycles the one with a lower residual amount not captured. The mmol of lanthanide captured per gram of sorbent after the first cycle and after the 9 cycles are reported in Table 1.

In this competitive interaction experiment involving La^{3+}, Gd^{3+} and Lu^{3+}, we observed a preferential uptake of Lu^{3+}, suggesting a stronger interaction with the sorbent material. Under competitive conditions, Lu^{3+} could not only bind more strongly but also effectively outcompetes the other lanthanides for the available sites, with a diminished ability to interact with the surface of La^{3+} and Gd^{3+} compared to isolated systems. Lu^{3+} being the smallest and therefore the one with the highest charge to radius ratio among the three lanthanides, can more readily displace hydration waters and approach the surface closely enough to form stable inner-sphere complexes. In contrast, La^{3+} ions tend to remain more solvated becoming less competitive in a mixed-ion environment, while Gd^{3+} position in between the two extremes being still outcompeted by Lu^{3+}. These findings underscore the antagonistic effects of a multi-component ion system, where differences in ionic radii and solvation energies can influence selective adsorption properties of materials.

Discussion

Among the REEs, the lanthanide series is considered one of the most valuable metals for a range of applications spanning from energy and green technologies to medical, electronics, defense and aerospace, industrial and catalytic applications. We selected three lanthanide elements for our adsorption tests with dioptase, i.e. gadolinium, lutetium and lanthanum. Gadolinium is a metal widely used in medicine for Magnetic Resonance Imaging (MRI) analyses. It is commonly employed

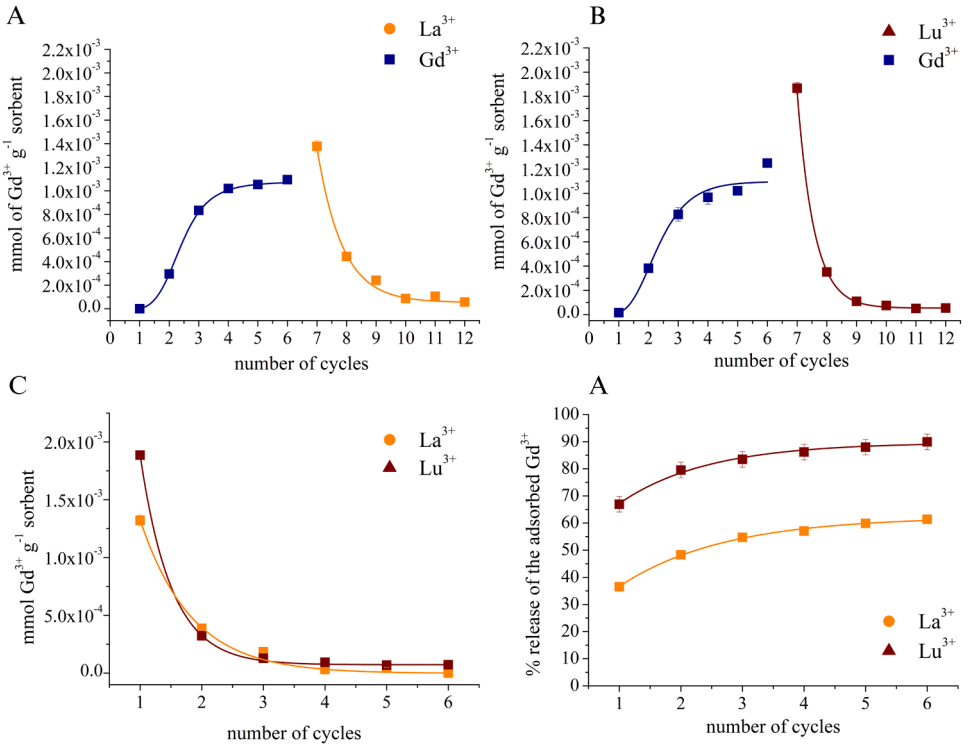


Fig. 9. A) In blue the adsorption profile of Gd^{3+}, in orange the La^{3+} induced desorption profile. B) In blue the adsorption profile of Gd^{3+}, in brown the Lu^{3+} induced desorption profile. Comparison of the Lu^{3+} or La^{3+} induced Gd^{3+} desorption profiles as mmol Gd^{3+} in C and as % of released Gd^{3+} over the previously adsorbed in D, orange for La^{3+} and brown for Lu^{3+}.

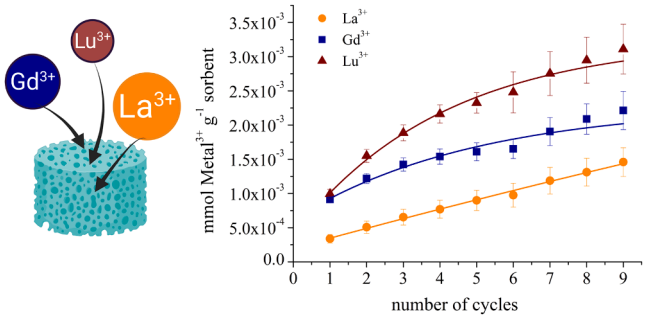


Fig. 10. Curves reporting the sum of the moles captured for every lanthanide, after each cycle, showing the different sorption profile of the three lanthanides, in orange La^{3+},in blue Gd^{3+} and in brown Lu^{3+}.

Table 1
mmol of lanthanides captured per g of material in the first cycle and after all the 9 cycles.

	mmol of metal captured after the first cycle (mmol g^{-1})	mmol of metal captured after the last cycle (mmol g^{-1})
Gadolinium	9.13×10^{-4}	2.21×10^{-3}
Lanthanum	3.39×10^{-4}	1.46×10^{-3}
Lutetium	9.92×10^{-4}	3.11×10^{-3}

in the form of linear or macrocyclic polyaminocarboxylate complexes as contrast agents (Gadolinium based contrast agents, GBCAs). In clinical diagnostic, GBCAs are normally intravenously administered at a dose of 0.1-0.4 mmol/kg. They have a short blood half-life (approximately 20 min) and, because of their low molecular weight and high hydrophilicity, are rapidly excreted through the kidneys into the urine. Following GBCA administration, urine collected during the first 24 h may contain gadolinium at concentrations substantially higher than those typically detected in environmental waters (*ca.* 2-4 mmol Gd/L in urine within 24 hours, *i.e.* in the millimolar range), whereas Gd concentrations in wastewater, rivers, lakes, and other aquatic environments are generally in the nanomolar range.

In the present study, a Gd^{3+} concentration of 0.1 mM was selected to enable reliable characterization of adsorption kinetics, uptake capacity, selectivity, and regeneration under well-controlled laboratory conditions. This concentration was not intended to reproduce a specific environmental or clinical scenario, but rather to provide a practical model system for investigating the adsorption behaviour of natural dioptase toward free lanthanide ions.

It should be noted that the proposed adsorption strategy is applicable only after the release of free lanthanide ions. Therefore, the treatment of GBCA-containing wastewaters requires a preliminary decomplexation step, such as advanced oxidation processes (AOPs) followed by acidification, which was not experimentally investigated in the present study. The validation of this integrated approach using pretreated and real wastewater matrices will be the subject of future investigations.

Within this framework, the present results provide the first systematic evaluation of the adsorption behaviour of natural dioptase toward free lanthanide ions, including adsorption kinetics, selectivity, regeneration capability, and structural stability. These fundamental data establish the basis for future investigations under more complex and application-oriented conditions. Future studies will also investigate the performance of dioptase using real hospital wastewater, municipal effluents, and environmental water samples, together with continuous-flow operation and techno-economic assessment, to evaluate the practical applicability of the proposed recovery strategy.

We investigated the potential of a natural mineral, dioptase, for metal removal from aqueous solutions. We began with a characterization of the cyclosilicate, followed by studies on the capture of Gd^{3+}, La^{3+}, and Lu^{3+} ions. The adsorption process was evaluated at different pH values (2.0 and 5.5). Lanthanide capture was monitored using

relaxometric measurements (^{1}H NMR, 0.5 T, 25°C), and the results were further validated by ICP-MS analysis using standardized metal and silicate concentrations. The first 24 hours of the adsorption process were monitored to determine the time at which nearly all the added metal was captured. Consequently, we chose 24 hours as the duration for each cycle to enhance the efficiency of subsequent cycles, repeating the adsorption process at least six times per saturation cycle. We decided to test whether a preconditioning treatment of the powder under acidic conditions (pH 2) could enhance the capture efficiency, as our analysis suggested that the release of non-structural Cu^{2+} in acid could increase the number of available sites for metal binding. Data showed no increase in adsorption capacity probably due to H_3O^+ competition for the same sites. Under the tested conditions, we found that the capture efficiency of Gd^{3+} ions after a single cycle is nearly 100%. Then we evaluated the desorption capacity of the silicate first subjected to repeated capture cycles. This metal loaded powders, were tested by placing them in a saturated NaCl solution, which resulted in negligible Gd^{3+} release. Then the tests were conducted under acidic conditions, which instead led to a moderate Gd^{3+} release. We further investigated the desorption mechanism by testing Gd^{3+}-loaded powder in the presence of an excess of La^{3+} or Lu^{3+}, maintaining a fixed 5000:1 weight ratio, to determine whether the powder preferentially binds metals according to a size-exclusion affinity process. We observed a higher affinity for the Lu^{3+} ions, with an adsorption that could be not only governed solely by ionic radius, but rather by charge density and hydration thermodynamics. Following the results, we tested the adsorption properties by putting in contact the sorbent powder with simultaneously the same amount of all the three lanthanides, finding again a preferential binding for Lu^{3+} ions confirming the hypothesis of a charge-to-size related preferential binding mechanism. Although its adsorption capacity does not surpass that of more efficient engineered materials reported in the literature (Table 2), considering its natural origin, structural stability, reversible metal release, and the possibility of repeated use, dioptase represents a promising low-processing alternative for sustainable rare-earth recovery applications.

However, the recovery and monitoring of metals in environmental matrices extend beyond aqueous-phase chemistry and represent an increasingly important challenge for environmental management. Future research should not only focus on optimizing the adsorption and regeneration performance of natural sorbents but also explore their integration with emerging technologies for the detection, monitoring, and discrimination of metals in complex environmental matrices. Although these approaches rely on different methodologies, their combination could support more efficient resource recovery, environmental monitoring, and sustainable management of critical raw (Khan et al., 2024).

Conclusions

In this study, we demonstrate, to the best of our knowledge, for the first time the use of dioptase as a natural sorbent for rare-earth element recovery by applying low-field ^{1}H-NMR relaxometry for real-time, non-destructive monitoring of lanthanide uptake. Dioptase achieved near-quantitative removal of Gd^{3+} from aqueous solution (99.6% within 7 h at pH 5.5, Kd = 641.3 mL g^{-1}), with adsorption kinetics best described by a diffusion-controlled parabolic model. Competition experiments revealed a selectivity order of $Lu^{3+} > Gd^{3+} > La^{3+}$, consistent with the effects of lanthanide contraction, ionic radius, and charge density, although the molecular adsorption mechanism requires further spectroscopic investigation. The material also showed remarkable structural stability over multiple adsorption/desorption cycles, with minimal release of non-structural Cu^{2+} ions and partial regeneration under acidic conditions.

Dioptase therefore represents a promising natural sorbent for the recovery of free lanthanide ions from aqueous media. However, the extension of this strategy to GBCA-containing wastewaters will require an appropriate pretreatment step to release free lanthanide ions prior to adsorption, and the validation of this integrated approach in real wastewater matrices remains the subject of future investigations.

The adsorption performance observed in this study, together with the absence of chemical modification or complex material synthesis, highlights the potential of natural dioptase as a sustainable alternative for rare-earth recovery. Beyond biomedical applications, this approach may also be relevant for the recovery of lanthanides from industrial and electronic waste streams, contributing to circular economy strategies and to reducing the environmental mobility of strategic metals. Future work will focus on validating the proposed approach using pretreated real wastewater matrices under continuous-flow conditions and evaluating its techno-economic feasibility for practical implementation.

Table 2
Comparison of different sorbent material as capacity of removing Gd^{3+} from the solution.

Sorbent	mmol Gd^{3+} / g sorbent	mg Gd^{3+} / g sorbent
Dioptase	1.33×10^{-3} (24 h) $5.25 \pm 0.07 \times 10^{-3}$ (8 cycles)	0.21 (24 h) 0.83 (8 cycles)
Synthetic saponite clay, Na-SAP-110[24]	$3.43 \times 10^{-3} \pm 1.27 \times 10^{-4}$ (5 h)	0.54 ± 0.02 (5 h)
Synthetic saponite clay, Na-SAP-20[24]	$3.56 \times 10^{-3} \pm 6.36 \times 10^{-5}$ (5 h)	0.56 ± 0.01 (5 h)
Mesoporous KZnFC ion exchange (Rizk et al., 2017)	3.50×10^{-3}	0.55
Na-MMT (Maza-Rodriguez et al., 1992)	0.3	47

Abbreviations

CN, Coordination Number; GBCAs, Gadolinium-Based Contrast Agents; ICP-MS, Inductively Coupled Plasma Mass Spectrometry; Kd, Distribution Coefficient;; MRI, Magnetic Resonance Imaging; R_1, Longitudinal Relaxation Rate; REEs, Rare Earth Elements; RT, Room Temperature; SEM, Scanning Electron Microscopy; SLE, Solid-Liquid Extraction; T_1, Longitudinal Relaxation Time; UV–Vis, Ultraviolet–Visible Spectroscopy; PXRD, Powder X-ray Diffraction;

Environmental implications

The rising rare earth elements (REEs) demand and environmental emissions into aquatic ecosystems through industrial effluents, medical waste streams, and urban wastewater systems, poses ecological risks and potential human health concerns due to their non-essential biological role and documented bioaccumulation and induced toxicity in various species. The natural copper cyclosilicate dioptase, offers an effective, economically viable solution for REEs recovery from contaminated water, achieving a near-complete removal of the tested species under mildly acidic conditions within 24 hours, with a reversible desorption of the trapped metals, that enable potential reuse and metal recycling, supporting circular economy principles.

CRediT authorship contribution statement

Angelo Scarciglia: Writing – review & editing, Writing – original draft, Methodology, Investigation, Formal analysis, Data curation, Conceptualization. **Francesco Rosario La Corte:** Investigation. **Marianna Sorrentino:** Investigation. **Stefano Marchesi:** Investigation. **Chiara Bisio:** Methodology. **Fabio Carniato:** Writing – review & editing, Writing – original draft, Supervision, Methodology. **Enza Di Gregorio:** Methodology, Funding acquisition. **Giuseppe Ferrauto:** Writing – review & editing, Writing – original draft, Supervision, Project administration, Methodology, Funding acquisition, Conceptualization.

Declaration of competing interest

The authors declare that they have no known competing financial interests or personal relationships that could have appeared to influence the work reported in this paper.

Acknowledgements

This publication is part of the NODES project (Nord Ovest Digitale e Sostenibile) which has received funding from the MUR – M4C2 1.5 of PNRR with grant agreement no. ECS00000036 (G.F.). The authors thank the NODES project - Spoke 2 "Green Technologies and Sustainable Industries" for its financial support. Fundings from Fondazione Cassa di Risparmio di Torino (CRT) are acknowledged. The authors acknowledge the Italian Ministry of Research for FOE contribution to the Euro-BioImaging MultiModal Molecular Imaging Italian Node (www.mmmi.unito.it). Some Figs. are created using BioRender.com. Associazione Italiana Ricerca sul cancro- AIRC- is gratefully acknowledged for the IG2025 IG, Rif. 32524 - Cellular Water cycling: A Biomarker of tumor metabolism in Breast Cancer Phenotyping and Therapeutic Monitoring Using MRI- P.I. Giuseppe Ferrauto.

Supplementary materials

Supplementary material associated with this article can be found, in the online version, at doi:10.1016/j.hazadv.2026.101424.

Data availability

Data will be made available on request.

References

A refinement of the structure of dioptase, Cu6[Si6O18].6H2O. https://pubs.geoscienceworld.org/msa/ammin/article-abstract/62/7-8/807/40807/A-refinement-of-the-structure-of-dioptase-Cu6.
Adsorption isotherms and kinetics. In: Interface Science and Technology, 33, 2021. Elsevier, pp. 445–509.
Abdullah, N., Yusof, N., Lau, W.J., Jaafar, J., Ismail, A.F., 2019. Recent trends of heavy metal removal from water/wastewater by membrane technologies. J. Ind. Eng. Chem. 76, 17–38.
Ament, L.J.P., Van Veenendaal, M., Devereaux, T.P., Hill, J.P., Van Den Brink, J., 2011. Resonant inelastic x-ray scattering studies of elementary excitations. Rev. Mod. Phys. 83, 705–767.
Ancora, G., et al., 2024. Silica-based monoliths functionalized with DTPA for the removal of transition and lanthanide ions from aqueous solutions. Dalton Trans. 53, 7801–7811.
Awual, Md.R., et al., 2017. Ligand field effect for Dysprosium(III) and Lutetium(III) adsorption and EXAFS coordination with novel composite nanomaterials. Chem. Eng. J. 320, 427–435.
Awual, M.R., et al., 2019. Introducing an amine functionalized novel conjugate material for toxic nitrite detection and adsorption from wastewater. J. Clean. Prod. 228, 778–785.
Awual, Md.R., et al., 2023. Green and robust adsorption and recovery of Europium(III) with a mechanism using hybrid donor conjugate materials. Sep. Purif. Technol. 319, 124088.
Birka, M., Roscher, J., Holtkamp, M., Sperling, M., Karst, U., 2016. Investigating the stability of gadolinium based contrast agents towards UV radiation. Water Res. 91, 244–250.
Brünjes, R., Hofmann, T., 2020. Anthropogenic gadolinium in freshwater and drinking water systems. Water Res. 182, 115966.
Chmielarz, L., Kuśtrowski, P., Dziembaj, R., Cool, P., Vansant, E.F., 2006. Catalytic performance of various mesoporous silicas modified with copper or iron oxides introduced by different ways in the selective reduction of NO by ammonia. Appl. Catal. B Environ. 62, 369–380.
Colombo, F., Lira, R., Ripley, E.M., González Del Tánago, J., 2012. Geology, mineralogy and possible origin of the copper mineralization in marble near Saldán, Córdoba (Argentina). J.Geosci. 299–316. https://doi.org/10.3190/jgeosci.102.
Cyris, M., et al., 2013. Reaction of gadolinium chelates with ozone and hydroxyl radicals. Environ. Sci. Technol. 47, 9942–9949.
D'Angelo, P., Spezia, R., 2012. Hydration of Lanthanoids(III) and Actinoids(III): an experimental/theoretical saga. Chem. – Eur. J. 18, 11162–11178.
D'Angelo, P., et al., 2011. Revised ionic radii of Lanthanoid(III) ions in aqueous solution. Inorg. Chem. 50, 4572–4579.
Dekker, H.M., Stroomberg, G.J., Van Der Molen, A.J., Prokop, M., 2024. Review of strategies to reduce the contamination of the water environment by gadolinium-based contrast agents. Insights Imag. 15, 62.
Edward, K., Yuvaraj, K.M., Kapoor, A., 2024. Chitosan-blended membranes for heavy metal removal from aqueous systems: a review of synthesis, separation mechanism, and performance. Int. J. Biol. Macromol. 279, 134996.
Elgoud, E.M.A., Ismail, Z.H., El-Nadi, Y.A., Abdelwahab, S.M., Aly, H.F., 2022. Solid–liquid extraction of rare Earth elements Ce(IV), Pr(III), Er(III), and Y(III) from concentrated phosphoric acid solutions using strongly acidic cation exchange resin (SQS–6). Russ. J. Appl. Chem. 95, 602–615.
Elmholdt, T.R., et al., 2011. Nephrogenic systemic fibrosis is found only among gadolinium-exposed patients with renal insufficiency: a case–control study from Denmark. Br. J. Dermatol. 165, 828–836.
Fei, Y., Hu, Y.H., 2023. Recent progress in removal of heavy metals from wastewater: A comprehensive review. Chemosphere 335, 139077.
Figueiredo, C., et al., 2021. Rare earth and trace elements in deep-sea sponges of the North Atlantic. Mar. Pollut. Bull. 166, 112217.
Gossuin, Y., Vuong, Q.L., 2018. NMR relaxometry for adsorption studies: proof of concept with copper adsorption on activated alumina. Sep. Purif. Technol. 202, 138–143.
Guerreiro, A., Brito, P., 2023. Stability of the macrocyclic Gd-DOTA contrast agent (DOTAREM) under different estuarine environmental conditions. Oceans 4, 381–393.
Gupta, A., et al., 2021. A review of adsorbents for heavy metal decontamination: growing approach to wastewater treatment. Materials 14, 4702.
Hadibarata, T., Syafrudin, M., Fitriyani, N.L., Lee, S.W., 2025. Advancements in composting technologies for efficient soil remediation of polycyclic aromatic hydrocarbons (PAHs): a mini review. Sustainability 17, 5881.
Hong, M., et al., 2019. Heavy metal adsorption with zeolites: the role of hierarchical pore architecture. Chem. Eng. J. 359, 363–372.
Idée, J., et al., 2009. Role of thermodynamic and kinetic parameters in gadolinium chelate stability. J. Magn. Reson. Imag. 30, 1249–1258.
Ilgen, A.G., Kabengi, N., Smith, J.G., Sanchez, K.M.M., 2023. Ion solvation as a predictor of lanthanide adsorption structures and energetics in alumina nanopores. Commun. Chem. 6, 172.
International Energy Agency (IEA). Rare Earth elements pathways to secure and diversified supply chains. (2026).
Islam, A., et al., 2025. Next frontier in photocatalytic hydrogen production through CdS heterojunctions. Int. J. Hydrog. Energy 101, 173–211.
Jordan, D.S., Malin, J.N., Geiger, F.M., 2010. Interactions of Al(III), La(III), Gd(III), and Lu(III) with the fused silica/water interface studied by second harmonic generation. Environ. Sci. Technol. 44, 5862–5867.
Khan, M.U., et al., 2024. Multi-sensor fusion for remote sensing of metallic and non-metallic object classification in complex soil environments and at different depths. IEEE Trans. Geosci. Remote Sens. 62, 1–13.
Kulaksız, S., Bau, M., 2011. Anthropogenic gadolinium as a microcontaminant in tap water used as drinking water in urban areas and megacities. Appl. Geochem. 26, 1877–1885.
Kumasaka, S., et al., 2024. Anthropogenic gadolinium in the Tone River (Japan): an update showing a 7.7-fold increase from 1996 to 2020. Eur. Radiol. Exp. 8, 64.
Law, J.M., Hoch, C., Whangbo, M., Kremer, R.K., 2010. Description of anhydrous (black) dioptase as a $S = 1/2$ uniform antiferromagnetic chain system. Z. Für Anorg. Allg. Chem. 636, 54–61.
Le Goff, S., et al., 2019. Compound-specific recording of gadolinium pollution in coastal waters by great scallops. Sci. Rep. 9, 8015.
Li, L., Shi, X., C, M., G, L., 2012. Atomic and molecular low-n rydberg states in near critical point fluids. In: Akhyar Farrukh, M. (Ed.), Advanced Aspects of Spectroscopy. InTech. https://doi.org/10.5772/50128.
Lundberg, D., Persson, I., Eriksson, L., D'Angelo, P., De Panfilis, S., 2010. Structural study of the *N,N′* -dimethylpropyleneurea solvated Lanthanoid(III) ions in solution and solid state with an analysis of the ionic radii of Lanthanoid(III) ions. Inorg. Chem. 49, 4420–4432.
Marchesi, S., et al., 2020. Synthetic saponite clays as promising solids for lanthanide ion recovery. New J. Chem. 44, 10033–10041.
Marchesi, S., Nascimbene, S., Guidotti, M., Bisio, C., Carniato, F., 2022. Application of NMR relaxometry for real-time monitoring of the removal of metal ions from water by synthetic clays. Dalton Trans. 51, 4502–4509.
Mariana, M., et al., 2021. Recent advances in activated carbon modification techniques for enhanced heavy metal adsorption. J. Water Process Eng. 43, 102221.
Martínez-Montoya, P.A., et al., 2024. Solid-liquid extraction for yttrium recovery using porous polymeric resin (XAD-7) functionalized with D2EHPA. J. Rare Earths 42, 1764–1773.
Martino, C., et al., 2018. Gadolinium perturbs expression of skeletogenic genes, calcium uptake and larval development in phylogenetically distant sea urchin species. Aquat. Toxicol. 194, 57–66.
Maza-Rodriguez, J., Olivera-Pastor, P., Bruque, S., Jimenez-Lopez, A., 1992. Exchange selectivity of lanthanide ions in montmorillonite. Clay Miner 27, 81–89.
Michałek, T., et al., 2025. Adsorption of Au(III), Pt(IV), Pd(II), and Rh(III) ions on activated carbon in a batch reactor supported by microwave radiation. Sci. Rep. 15, 5852.
Miller, M., Chu, M., Lin, B., Bu, W., Dutta, P., 2017. Atomic number dependent "structural transitions" in ordered lanthanide monolayers: role of the hydration shell. Langmuir 33, 1412–1418.
Mindat. Dioptase. (2026).

Morton, L.D., et al., 2025. Mechanically and chemically robust lanmodulin-functionalized silk sponges for rare Earth element sequestration. ACS Biomater. Sci. Eng. 11, 4076–4086.
Mosai, A.K., Chimuka, L., Cukrowska, E.M., Kotzé, I.A., Tutu, H., 2019. The recovery of rare Earth elements (REEs) from aqueous solutions using natural zeolite and bentonite. Water. Air. Soil Pollut. 230, 188.
Mugion, R.G., Elmo, G.C., Ungaro, V., Di Pietro, L., Martucci, O., 2025. A systematic literature review of selected aspects of life cycle assessment of rare earth elements: integration of digital technologies for sustainable production and recycling. Sustainability 17, 5825.
Ogata, T., Narita, H., 2024. Separation of adjacent light rare Earth elements using silica gel modified with diglycolamic acid. Materials 17, 2648.
Qiu, L., et al., 2022. Adsorption of heavy metals by activated carbon: effect of natural organic matter and regeneration methods of the adsorbent. Desalination Water Treat 252, 148–166.
Raji, Z., Karim, A., Karam, A., Khalloufi, S., 2023. Adsorption of heavy metals: mechanisms, kinetics, and applications of various adsorbents in wastewater remediation—a review. Waste 1, 775–805.
Reddy, K.M., Jacob, A.S., Reddy, B.J., 1986. EPR and optical spectra of Cu^{2+} in dioptase. Ferroelectr. Lett. Sect. 6, 103–112.
Rizk, H.E., Attallah, M.F., Ali, A.M.I., 2017. Investigations on sorption performance of some radionuclides, heavy metals and lanthanides using mesoporous adsorbent material. J. Radioanal. Nucl. Chem. 314, 2475–2487.
Rudolph, W.W., Irmer, G., 2020. On the hydration of the Rare Earth ions in aqueous solution. J. Solut. Chem. 49, 316–331.
Scarciglia, A., et al., 2025. Gadolinium-based contrast agents (GBCAs) for MRI: a benefit–risk balance analysis from a chemical, biomedical, and environmental point of view. Glob. Chall. 9, 2400269.
Sen Gupta, S., Bhattacharyya, K.G., 2011. Kinetics of adsorption of metal ions on inorganic materials: a review. Adv. Colloid Interface Sci. 162, 39–58.
Shahat, A., Kubra, K.T., Salman, Md.S., Hasan, Md.N., Hasan, Md.M., 2021. Novel solid-state sensor material for efficient cadmium(II) detection and capturing from wastewater. Microchem. J. 164, 105967.
Sijl, J.van, 2011. Trace Elements in High Pressure and Temperature Fluids in Subduction Zones. Vrije Universiteit, Amsterdam.
Tansel, B., et al., 2006. Significance of hydrated radius and hydration shells on ionic permeability during nanofiltration in dead end and cross flow modes. Sep. Purif. Technol. 51, 40–47.
Waliullah, R.M., et al., 2023. Optimization of toxic dye removal from contaminated water using chitosan-grafted novel nanocomposite adsorbent. J. Mol. Liq. 388, 122763.
Werner, P., et al., 2022. Investigating the role of sulfate groups for the binding of Gd^{3+} ions to glycosaminoglycans with NMR relaxometry. ChemMedChem 17, e202100764.
Wijesinghe, S., Dittrich, T.M., Allen, M.J., 2026. Sustainable strategy for preventing medical gadolinium from entering surface water. Npj Emerg. Contam. 2, 14.
Xu, T., et al., 2024. Green recovery of rare earth elements under sustainability and low carbon: a review of current challenges and opportunities. Sep. Purif. Technol. 330, 125501.
Zepf, V., 2016. An overview of the usefulness and strategic value of rare Earth metals. In: Rare Earths Industry, 3–17. Elsevier. https://doi.org/10.1016/B978-0-12-802328-0.00001-2.
Zhang, H., Pan, D., Duan, X., 2009. Synthesis, characterization, and magnetically controlled release behavior of novel core−shell structural magnetic ibuprofen-intercalated LDH nanohybrids. J. Phys. Chem. C 113, 12140–12148.
Zhang, S., Kano, N., Mishima, K., Okawa, H., 2019. Adsorption and desorption mechanisms of rare Earth elements (REEs) by layered double hydroxide (LDH) modified with chelating agents. Appl. Sci. 9, 4805.
Zhang, Q., O'Brien, S., Grimm, J., 2022. Biomedical applications of lanthanide nanomaterials, for imaging, sensing and therapy. Nanotheranostics 6, 184–194.
Zhang, J., et al., 2025. Selective recovery of rare earth elements from mine wastewater using the magnetic zeolite prepared by rare earth tailings. Chem. Eng. J. 511, 161871.
Zhang, Y., Idota, N., Tsukahara, T., 2025. Surface-functionalized polydimethylsiloxane sponges for facile and selective recovery of molybdenum from aqueous/acidic solutions. J. Hazard. Mater. 488, 137485.
Zhang, L., Chen, C., Zhou, C., Luo, Y., Wu, X., 2025. Zone-based many-objective building decarbonization considering outdoor temperature and occupation uncertainty. Renew. Sustain. Energy Rev. 208, 115003.